

Voxel Based Analysis of Diffusion Indices in Patients with Primary Open-Angle Glaucoma Using Tract-Based Spatial Statistics

Manuel A. Schmidt^{1*}, Sultan Haider^{3,4,6#}, Angelika Mennecke¹, Richard Johnson⁴, Joachim Hornegger^{3,4,5}, Georg Michelson², Arnd Doerfler¹ and Tobias Engelhorn¹

¹Department of Neuroradiology, University of Erlangen-Nuremberg, Germany

²Department of Ophthalmology, University of Erlangen-Nuremberg, Germany

³Pattern Recognition Lab, University of Erlangen-Nuremberg, Germany

⁴Central Institute of Medical Engineering, University of Erlangen-Nuremberg, Germany

⁵Erlangen Graduate School in Advanced Optical Technologies (SAOT), University of Erlangen-Nuremberg, Germany

⁶Siemens Healthcare, Erlangen, Germany

#These authors contributed equally to this work and thus share first authorship.

*Corresponding author: Manuel A. Schmidt, MD, Department of Neuroradiology, Friedrich-Alexander-University Erlangen-Nuremberg, Schwabachanlage 6, 91054 Erlangen, Germany, Tel: +49 9131 85 44821; Fax: +49 9131 85 36179; Email: manuel.schmidt@uk-erlangen.de

Received date: Feb 05, 2015, Accepted date: Mar 26, 2015, Published date: Mar 30, 2015

Copyright: © 2015 Schmidt MA, et al. This is an open-access article distributed under the terms of the Creative Commons Attribution License, which permits unrestricted use, distribution, and reproduction in any medium, provided the original author and source are credited.

Abstract

Background and purpose: Diffusion tensor imaging can provide information about microstructural changes of the visual pathway in glaucoma patients. Tract-based spatial statistics (TBSS) has been established for analysis of fractional anisotropy (FA) and has successfully been used for analysis of DTI data of glaucoma patients. However there are certain DTI indices such as mean diffusivity (MD), radial diffusivity (RD), axial diffusivity (AD) and mode of anisotropy (MO), which can also be analyzed using TBSS. Hence, we tested whether TBSS is useful for analysis of non-FA data in glaucoma patients and for identification of microstructural changes in patients with primary open-angle glaucoma characterized by these non-FA DTI indices.

Material and methods: Our study comprised 46 patients with primary open-angle glaucoma (POAG) and a healthy, age-matched control group of 23 subjects. TBSS was used for analysis of FA as well as MO, MD, RD and AD.

Results: For an automated analysis of non-FA diffusion indices we could establish a workflow using TBSS in addition to its primary purpose, the analysis of FA. Our results reveal clusters of voxels with overlapping decreased FA and increased RD and MD in the optic radiation as well as in visual association tracts.

Conclusion: TBSS is a useful tool not only for analysis of FA but also of non-FA diffusion indices in glaucoma patients. Overlapping decreased FA and increased MD and RD can be found in POAG patients not only in the optic radiation but also in visual association tracts, suggestive for significant neurodegeneration in POAG.

Keywords Tract-based spatial statistics; Primary open-angle glaucoma; DTI; Fractional anisotropy; Diffusion indices; Mode of anisotropy; Radial diffusivity; Mean diffusivity; Axial diffusivity

Introduction

Magnetic resonance diffusion imaging has been used to analyze the visual pathway in glaucoma [1-3]. A tensor model fit to diffusion MRI data provides scalar measurements to perform voxel wise analysis of white matter properties [4]. As glaucoma is more and more comprehended as a neurodegenerative disease, advanced imaging post processing algorithms have been developed for sophisticated analysis of diffusion indices, primarily fractional anisotropy (FA) [5-7].

Tract-based spatial statistics (TBSS) can help to solve crucial issues of spatial alignment, allowing non-biased whole brain cross-subject statistical analysis [8]. In addition to FA, several diffusion indices have been described to be associated with distinct microstructural changes of white-matter tracts: mean diffusivity (MD) is thought to represent cell membrane degradation [9] and demyelination has been shown to be represented by radial diffusivity (RD) [10]. Non-FA diffusion indices have been analyzed with statistical parametric mapping [11]. However there is only one study [12] that conducted a TBSS based analysis; this study comprised only a small amount of patients and performed no analysis of MD and another important diffusion measure, mode of anisotropy.

Thus, the aim of this study was to establish an automated workflow for whole brain analysis of multiple diffusion indices in glaucoma

patients and to identify and assess microstructural changes that are represented by changes of diffusion measures compared to healthy, age-matched control individuals.

Material and Methods

Subjects

This retrospective study included 69 subjects comprising 46 severely affected patients with primary open-angle glaucoma (POAG,

intraocular pressure of both eyes prior to treatment ≥ 22 mmHg; mean age=63.75 years ± 10.79) and a healthy, age-matched control group of 23 subjects (CONT, mean age=59.54 years ± 14.06). The individuals of the CONT group underwent full ophthalmological examination to exclude an intraocular pressure ≥ 22 mmHg, optic nerve head atrophy and visual disturbances. Patients' characteristics are summarized in Table 1. The Clinical Investigation Ethics Committee of the University of Erlangen-Nuremberg approved the study protocol and the research was conducted in accordance with the Declaration of Helsinki and informed consent was obtained from all subjects.

| POAG +/- SD (standard value) | Right eye | Left eye |
|--|-------------------|-------------------|
| HRT disc area (1.69-2.82 mm ²) | 2.326 \pm 0.596 | 2.353 \pm 0.643 |
| HRT cup area (0.26-1.27 mm ²) | 1.051 \pm 0.512 | 1.108 \pm 0.611 |
| HRT rim area (1.2-1.78 mm ²) | 1.276 \pm 0.511 | 1.246 \pm 0.613 |
| RNFL thickness (0.18-0.31 mm) | 0.194 \pm 0.062 | 0.194 \pm 0.124 |
| FDT duration (≤ 50 s) | 66.7 \pm 34.8 | 72.0 \pm 33.0 |

Table 1: Clinical characteristics of POAG patients. HRT:Heidelberg Retina Tomograph; RNFL:Retina Fiber Layer Thickness; FDT:Frequency Doubling Test

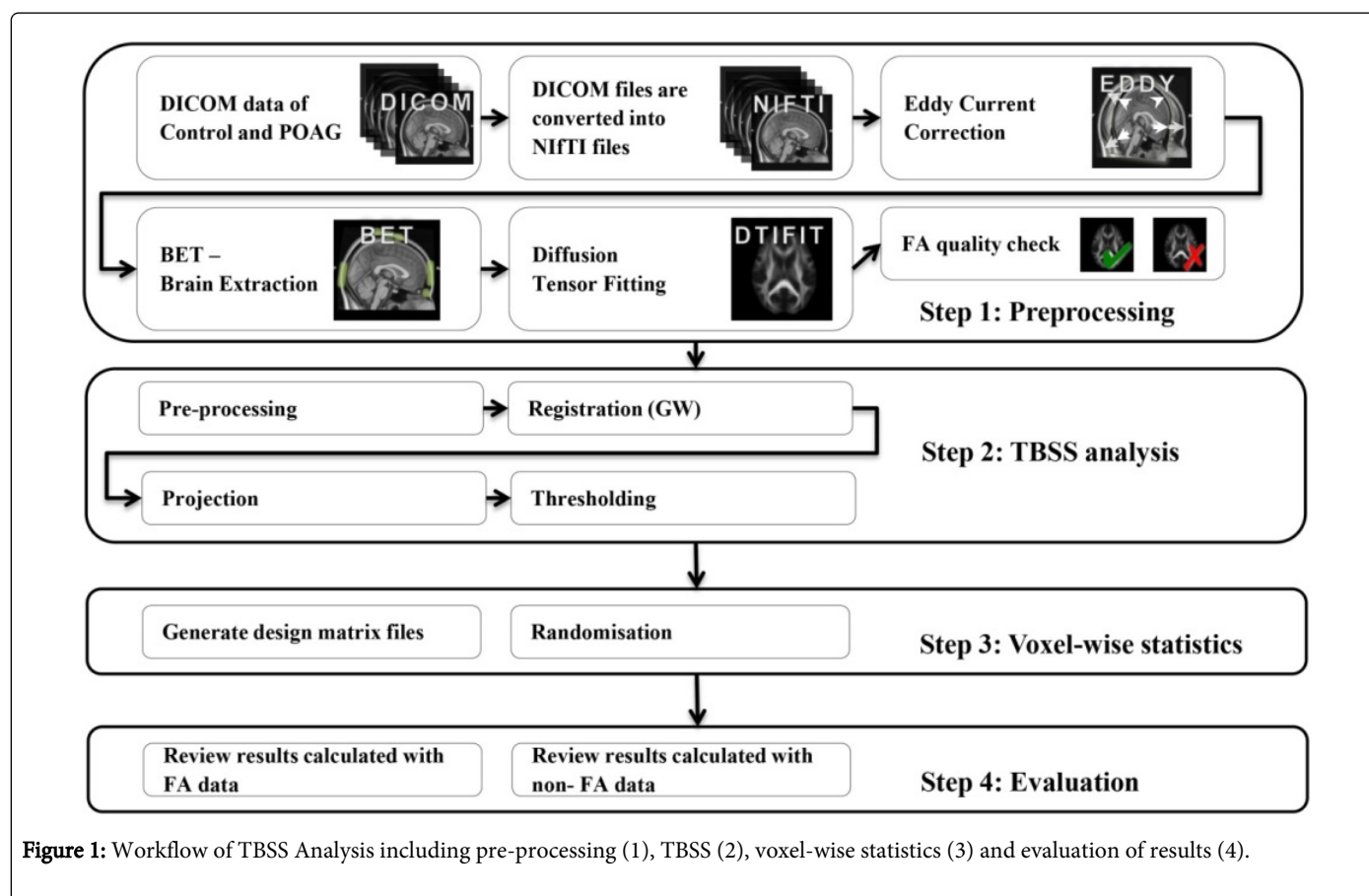


Figure 1: Workflow of TBSS Analysis including pre-processing (1), TBSS (2), voxel-wise statistics (3) and evaluation of results (4).

MRI Sequence

A 3T high-field scanner (Magnetom Tim Trio, Siemens Healthcare AG, Erlangen, Germany) with gradient field strength up to 45 mT/m

(72 mT/m effective) was used. DTI was performed in the axial plane with 4 mm slice thickness using a single-shot, spin echo, echo planar imaging (EPI) diffusion tensor sequence (TR=3400 ms, TE=93 ms, FoV=230 \times 230 mm², acquisition matrix size=256 \times 256 reconstructed

to 512×512 , number of signal averages=7, partial Fourier acquisition=60%). Diffusion weighting was carried out with a maximal b-factor of 1000 s/mm^2 along 15 icosahedral directions complemented by one scan with $b=0$.

Image processing and TBSS analysis

The entire image processing and analysis workflow is pictured in Figure 1 and consisted of four steps: (1) Image preprocessing to set up DTI data for tract-based spatial statistics (TBSS), (2) run TBSS, (3) voxel wise statistical analysis and (4) examination and review of results.

Voxel wise statistical analysis of FA was carried out using TBSS [5], part of FSL, a comprehensive library of analysis tools for FMRI, MRI and DTI brain imaging data [13,14]. For Preprocessing DICOM images were converted to NIFTI files (neuroimaging informatics technology initiative) using `dcm2nii` from the MRICron-package (<http://www.mccauslandcenter.sc.edu/mricro/mricron/dcm2nii.html>).

The resulting images were then preprocessed for TBSS analysis, i.e. corrected for eddy currents and brain extracted with `bet` [15]. We chose a `bet2`-threshold of 0.2 to remove all non-brain tissue. Next a diffusion tensor model was fit at each voxel to extract the FA, MO, MD and AD maps using DTIFIT. All of these preprocessing steps were carried out using FMRIB diffusion toolbox (FDT) which is also part of FSL (<http://fsl.fmrib.ox.ac.uk/fsl>) [14].

During registration, mean FA skeletons were created using the registration to a group wise template (GW) as proposed in [7]. GW was used with 5 affine and 15 non-linear, gradually converging registration-steps and the mean FA skeleton image was thresholded to 0.2. Within the next step, the final transforms found in the previous stage were applied to all subjects to bring them into standard space.

After that, the mean FA image was skeletonized and regarding every individual FA image, the maximum FA values perpendicular to the mean skeleton were projected on the mean skeleton.

This step resulted in a 4D skeletonized FA image, comprising the individual skeletonized FA images. It was used to feed into voxel wise statistics and to observe which FA skeleton voxels are significantly different between the two groups of subjects.

Voxelwise statistics was performed using a two sample t-test with the permutation function randomise included in FSL, number of permutations set to 5000 and threshold-free cluster enhancement, fully corrected for multiple comparisons across space, with $p < 0.05$ resulting and 2 contrasts (CONT>POAG and CONT<POAG) [13,16].

Additionally to FA, TBSS evaluation was applied by this means to non-FA diffusion indices, obtained in the preprocessing step by DTIFIT. This included mean diffusivity ($MD = \frac{\lambda_1 + \lambda_2 + \lambda_3}{3}$), axial

diffusivity ($AD = \lambda_1$), radial diffusivity ($RD = \frac{\lambda_2 + \lambda_3}{2}$, calculated with `fslmaths`, a FSL command line utility) and mode of anisotropy (MO). MO describes the shape of the diffusion tensor. It ranges from -1 to +1 and gives complementary information to FA, as the shape ranges from more planar ($\lambda_1 \sim \lambda_2 \sim \lambda_3$, e.g. in areas of crossing fibers) to linear ($\lambda_1 > \lambda_2 \sim \lambda_3$, e.g. areas with one dominating fiber orientation) [16,17].

The data was processed referring to the calculated FA skeleton from group-wise registration. Voxelwise statistics with randomise (FSL's

tool for nonparametric permutation inference) were carried out in same manner as for FA (see above).

JHU white-matter tractography atlas was used for annotation [18,19].

Two experienced neuroradiologists performed evaluation of the results.

Results

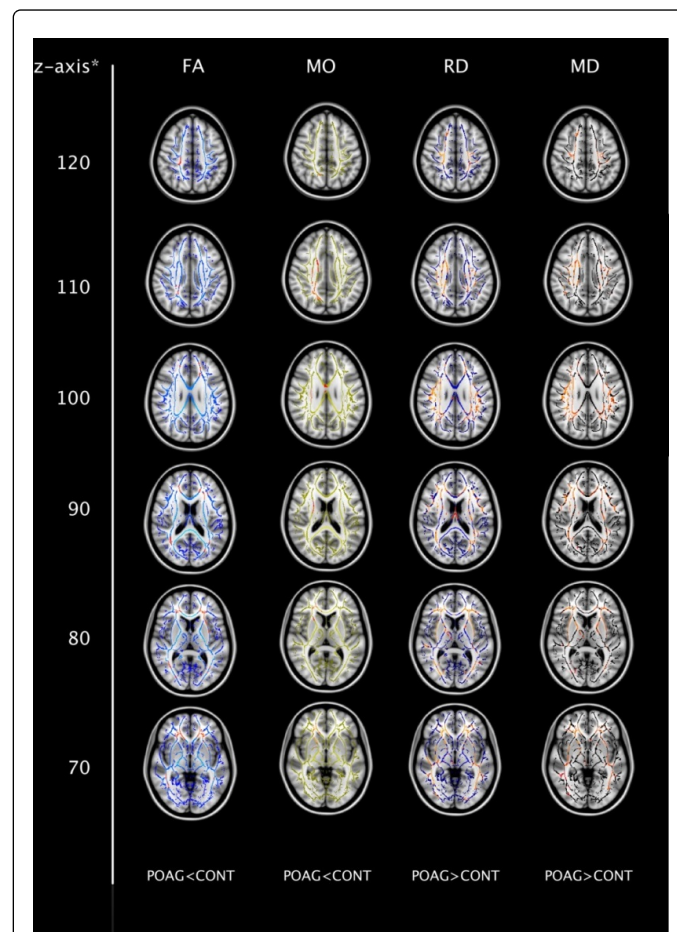


Figure 2: Mean FA skeleton overlaid onto the MNI152 standard template for anatomical orientation. Clusters of voxels of significantly decreased FA and MO and increased MD and RD values of POAG patients compared to controls are marked red ($p < 0.05$, corrected for multiple comparisons). *Z-axis in MNI_152 space.

We found clusters of voxels with decreased FA and MO and increased RD and MD in and outside the visual pathway in POAG compared to controls.

POAG patients exhibited decreased FA in the optic radiation bilaterally as well as in the right corticospinal tract, left anterior thalamic radiation, the corpus callosum and in association tracts, specifically the inferior fronto-occipital fasciculus (bilateral), the right superior and the inferior longitudinal fasciculus (bilateral) and the uncinate fasciculus (bilateral). MO was significantly decreased in the right corticospinal tract and superior corona radiata, right internal

capsule and anterior thalamic radiation and in the right uncinate fasciculus and inferior fronto-occipital fasciculus. There were no clusters of voxels with increased FA or MO in POAG patients compared to healthy controls.

RD and MD were increased in nearly all association tracts as well as in projection and commissural fibers. Cluster size and spatial distribution matched to a great extent for RD and MD (Figure 2). For contrast number 2, there were no voxels with decreased RD or MD in POAG patients.

We could not observe significant changes in axial diffusivity. Results are summarized in Table 1.

For the optic radiation we found decreased FA and overlapping increased MD and RD respectively (Figure 3). This was less pronounced for other projection fibers but could also be found in important association tracts related to the visual system.

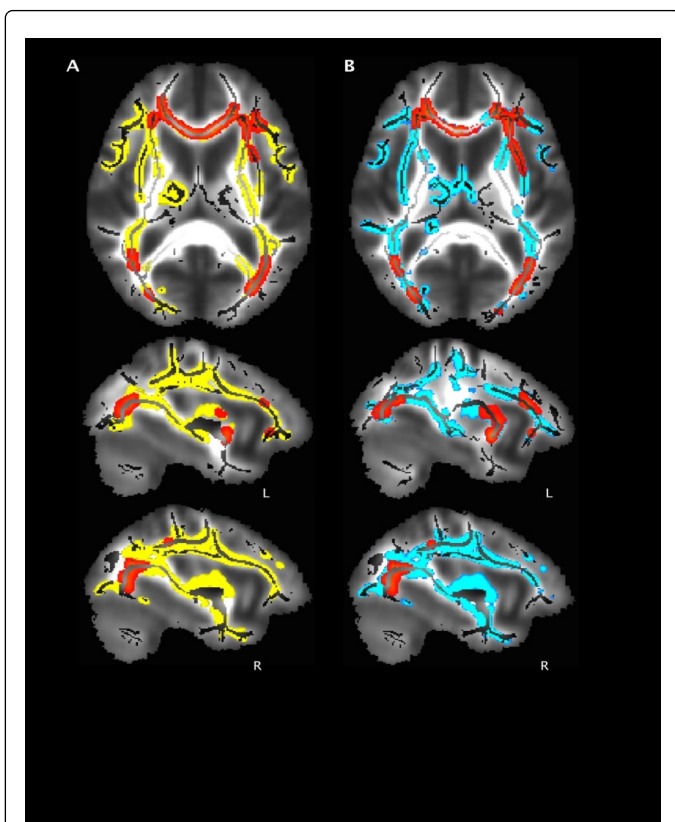


Figure 3: Mean FA skeleton overlaid onto the mean FA image. Tracts with overlapping decreased FA* (red) and a) increased MD* (yellow) b) increased RD* (blue). * $p < 0.05$, corrected for multiple comparisons.

Discussion

The aim of this study was to evaluate an automatized approach for analyzing FA and non-FA diffusion indices in POAG patients using TBSS. Therefore we optimized the TBSS pipeline for analysis of patients with a potentially neurodegenerative disease, as it has previously been shown, that brain atrophy has to be taken into account concerning the registration process [7,16,20].

Our results reveal decreased FA in POAG patients in the bilateral optic radiation as well as in association tracts linked to the visual pathway. Furthermore, we show that significant and widespread alteration of diffusion indices, especially MD and RD, in POAG patients compared to healthy control individuals is not limited to the visual pathway but can also be found in projection, association and commissural fibers.

Interestingly, overlapping of decreased FA and increased MD and RD could be found in the bilateral optic radiation as well as in important association fibers for processing of visual information indicating advanced neurodegeneration in POAG patients.

Decreased FA could be found in the bilateral optic radiation in POAG patients, which has previously been described [6,7]. Moreover, we found decreased FA in medial prefrontal association fibers, predominantly the superior and inferior longitudinal fasciculus, the inferior fronto-occipital fasciculus and uncinate fasciculus. The inferior fronto-occipital fasciculus connects the frontal region with inferior and dorsal parietal and occipital areas as an intrahemispheric association fiber running in sagittal orientation. The superior longitudinal fasciculus connects frontotemporal and frontoparietal regions. Both have been described to play a role in visual spatial processing [21] and whilst being affected by degeneration through decreased FA may contribute to visual impairment of patients.

The inferior longitudinal fasciculus runs from the frontal to the ipsilateral occipital lobe and interruption may lead to visual neglect and has been reported to be particularly involved in visual memory [22].

Resection of the uncinate fasciculus in glioma patients has led to a loss of performance in famous face naming [23] and it has been reported to be associated with visual associative learning suggesting that degeneration of the uncinate fasciculus may also be somewhat involved in the pathogenesis of glaucoma.

Our results are in line with previous reports that described reduced gray matter in POAG patients in the calcarine fissure, the postcentral gyrus, the superior frontal gyrus and the inferior frontal gyrus [24].

We found decreased mode of anisotropy values in the right corticospinal tract as well as in the superior corona radiata and the internal capsule and the right anterior thalamic radiation. Additionally, MO was significantly lower partly in the right inferior fronto-occipital and uncinate fasciculus and in the corpus callosum. The mode of anisotropy reflects the shape of the diffusion tensor, ranging from linear to planar. Lower mode of anisotropy indicates more planar diffusion, e.g. in areas of crossing fibers [17]. Reduced FA has been reported in such areas of crossing fibers and may in those cases not be due to axonal degradation but reflect disorganization of white-matter tracts [16]. The absence of decreased MO in the optic radiation and at least partly, in association tracts of the visual pathway, where we found markedly decreased FA values, may thus represent “true” FA reduction due to loss of axonal integrity.

While FA describes overall white matter integrity [9], increased MD (also known as ADC, apparent diffusion coefficient) has been linked to tissue breakdown due to cell membrane degeneration and is associated with increased brain water content [9,25]. We found increased MD in nearly all association tracts as well as in projection and commissural fibers.

Interestingly, overlapping of increased MD and decreased FA was markedly pronounced in the optic radiation and in those association

tracts, which are strongly connected to the visual system, like the inferior fronto-occipital fasciculus and superior longitudinal fasciculus (Figure 3).

In a cohort of patients with Alzheimer’s disease, overlapping changes in FA and MD have been reported to be due to gross tissue loss. This might also apply for glaucoma patients and may be a better indicator of white-matter degeneration as decreased FA alone.

Additionally, decrease in RD followed the decrease of MD to a great extent. Decreased RD has been associated with loss of myelin in animal studies [10] and has also been described in patients with Alzheimer’s disease [26,27] and in glaucoma [28]. Thus the overlapping of increased MD and RD with decreased FA is suggestive for advanced neurodegeneration in the optic radiation as well as in association tracts necessary for adequate processing of visual information in glaucoma patients.

For AD, there were also clusters of voxels with increased values in POAG patients, however, those clusters scarcely failed to reach statistical significance. This may be due to dynamic changes, which have been observed regarding axial diffusivity [29] (Table 2).

| | FA | MO | RD | MD |
|--|---------|---------|---------|---------|
| Projection fibers | | | | |
| Right corticospinal tract | x (120) | x (110) | x (120) | x (120) |
| Left corticospinal tract | | | x (120) | x (120) |
| Right superior corona radiata | | x (110) | x (120) | x (120) |
| Left superior corona radiata | | | x (120) | x (120) |
| Right posterior thalamic radiation (incl. optic radiation) | x (90) | | x (90) | x (90) |
| Left posterior thalamic radiation (incl. optic radiation) | x (90) | | x (90) | x (90) |
| Right anterior thalamic radiation | | x (80) | x (80) | x (90) |
| Left anterior thalamic radiation | x (90) | | x (80) | x (90) |
| Right internal capsule | | x (80) | x (80) | x (80) |
| Left internal capsule | | | x (80) | x (80) |
| Right capsula externa | | | x (80) | x (80) |
| Left capsula externa | | | x (80) | x (80) |
| Association fibers | | | | |
| Right superior longitudinal fasciculus | x (110) | | x (100) | x (100) |
| Left superior longitudinal fasciculus | | | x (100) | x (100) |
| Right inferior longitudinal fasciculus | x (80) | | x (80) | x (80) |
| Left inferior longitudinal fasciculus | x (80) | | x (80) | x (80) |
| Right inferior fronto-occipital fasciculus | x (100) | x (70) | x (80) | x (90) |
| Left inferior fronto-occipital fasciculus | x (100) | | x (80) | x (90) |

| | | | | |
|---------------------------|---------|---------|---------|--------|
| Right uncinata fasciculus | x (70) | x (70) | x (70) | x (70) |
| Left uncinata fasciculus | x (70) | | x (70) | x (70) |
| Commissural fibers | | | | |
| Forceps minor right | x (100) | x (80) | x (90) | x (70) |
| Forceps minor left | x (100) | | x (90) | x (80) |
| Genu of corpus callosum | x (80) | x (80) | x (80) | x (80) |
| Body of corpus callosum | | x (100) | x (120) | |
| Forceps major right | | | x (90) | x (90) |
| Forceps major left | | | | |

Table 2: White matter tracts with clusters of voxels of significantly decreased FA values, decreased mode of anisotropy, increased radial and mean diffusivity in POAG patients compared to controls (p<0.05, corrected for multiple comparisons), respectively. Coordinate of z-axis in brackets.

Glaucoma has commonly been understood as a disease affecting primarily the optic nerve, i.e. the third neuron of the visual pathway. However, as diffusion tensor imaging is more and more used not just for evaluation of the extracranial but also of the intracranial part of the visual pathway [1,30], the idea of a solely affected optic nerve in glaucoma has to be questioned. It has already been proposed that at least in some glaucoma patients a primary degeneration of the fourth neuron of the visual pathway, i.e. the optic radiation, might strongly contribute to disease pathogenesis rather than a secondary affection of the fourth neuron due to transsynaptic degeneration [31].

Our results suggest that neurodegeneration in POAG patients goes far beyond degeneration of the third and fourth neuron of the visual pathway. Decreased FA with simultaneously increased MD and RD is a strong indicator for advanced neurodegeneration in primary open-angle glaucoma. The described findings lead to the hypothesis that degeneration of visual association tracts is secondary to the initial degeneration of visual projection fibers, first to fourth neuron, rather than degeneration of the fourth neuron being secondary due to optic nerve atrophy. This notion would be in line with previous reports of an initial injury of the fourth neuron in primary open-angle glaucoma [31].

Disease severity in glaucoma is estimated by a profound ophthalmological examination, e.g. optic nerve head morphology or retinal nerve fiber layer thickness, in clinical practice. DTI of the central visual pathway may contribute to a better overall estimation of disease severity in POAG patients. At least for the optic radiation changes in FA, MD and RD have been shown to correlate with glaucoma severity [28].

Further studies are required to assess changes of these diffusion parameters in visual association tracts with regard to disease severity. Given that an impaired axonal integrity in tracts crucial for processing of visual information leads to an impaired visual field over time, it even seems possible to use DTI of the central visual pathway for an early detection of disease progress, before degeneration has reached the optic nerve or the retina, respectively.

It seems that, at least in certain glaucoma subtypes, i.e. primary open-angle glaucoma, the classical understanding of the pathogenesis

has to be rethought, as of glaucoma being a complex neurodegenerative disease.

Conclusion

TBSS is a useful tool not only for analysis of FA but also non-FA diffusion indices in glaucoma patients. Concurrent analysis of different DTI derived indices may provide a better pathophysiological understanding of primary open-angle glaucoma, as overlapping alterations of DTI indices suggest POAG to be a complex neurodegenerative disorder.

References

1. Engelhorn T, Michelson G, Waerntges S, Struffert T, Haider S, et al. (2011) Diffusion tensor imaging detects rarefaction of optic radiation in glaucoma patients. *Acad Radiol* 18: 764-769.
2. El-Rafei A, Engelhorn T, Warntges S, Dorfler A, Hornegger J, Michelson G. (2011) A framework for voxel-based morphometric analysis of the optic radiation using diffusion tensor imaging in glaucoma. *Magn Reson Imaging* 29: 1076-1087.
3. Hernowo AT, Boucard CC, Jansonius NM, Hooymans JM, Cornelissen FW (2011) Automated morphometry of the visual pathway in primary open-angle glaucoma. *Invest Ophthalmol Vis Sci* 52: 2758-2766.
4. Jbabdi S, Behrens TE, Smith SM (2010) Crossing fibres in tract-based spatial statistics. *Neuroimage* 49: 249-256.
5. Smith SM, Jenkinson M, Johansen-Berg H, Rueckert D, Nichols TE, et al. (2006) Tract-based spatial statistics: voxelwise analysis of multi-subject diffusion data. *NeuroImage* 31: 1487-505.
6. Lu P, Shi L, Du H, Xie B, Li C, et al. (2013) Reduced white matter integrity in primary open-angle glaucoma: a DTI study using tract-based spatial statistics. *J Neuroradiol* 40: 89-93.
7. Schmidt MA, Mennecke A, Michelson G, Doerfler A, Engelhorn T (2014) DTI analysis in patients with primary open-angle glaucoma: impact of registration on Voxel-Wise statistics. *PLoS One* 9: e99344.
8. Smith SM, Johansen-Berg H, Jenkinson M, Rueckert D, Nichols TE, et al. (2007) Acquisition and voxelwise analysis of multi-subject diffusion data with tract-based spatial statistics. *Nat Protoc* 2: 499-503.
9. Pierpaoli C, Basser PJ (1996) Toward a quantitative assessment of diffusion anisotropy. *Magnetic resonance in medicine* 36: 893-906.
10. Song SK, Sun SW, Ramsbottom MJ, Chang C, Russell J, et al. (2002) Demyelination revealed through MRI as increased radial (but unchanged axial) diffusion of water. *Neuroimage* 17: 1429-1436.
11. Dai H, Yin D, Hu C, Morelli JN, Hu S, et al. (2013) Whole-brain voxel-based analysis of diffusion tensor MRI parameters in patients with primary open angle glaucoma and correlation with clinical glaucoma stage. *Neuroradiology* 55: 233-243.
12. Frezzotti P, Giorgio A, Motolese I, De Leucio A, Iester M, et al. (2014) Structural and functional brain changes beyond visual system in patients with advanced glaucoma. *PLoS One* 9: e105931.
13. Smith SM, Jenkinson M, Woolrich MW, Beckmann CF, Behrens TE, et al. (2004) Advances in functional and structural MR image analysis and implementation as FSL. *Neuroimage* 23 Suppl 1: S208-219.
14. Jenkinson M, Beckmann CF, Behrens TE, Woolrich MW, Smith SM (2012) FSL. *Neuroimage* 62: 782-790.
15. Smith SM (2002) Fast robust automated brain extraction. *Hum Brain Mapp* 17: 143-155.
16. Douaud G, Jbabdi S, Behrens TE, Menke RA, Gass A, et al. (2011) DTI measures in crossing-fibre areas: increased diffusion anisotropy reveals early white matter alteration in MCI and mild Alzheimer's disease. *Neuroimage* 55: 880-890.
17. Ennis DB, Kindlmann G (2006) Orthogonal tensor invariants and the analysis of diffusion tensor magnetic resonance images. *Magn Reson Med* 55: 136-146.
18. Wakana S, Caprihan A, Panzenboeck MM, Fallon JH, Perry M, et al. (2007) Reproducibility of quantitative tractography methods applied to cerebral white matter. *Neuroimage* 36: 630-644.
19. Hua K, Zhang J, Wakana S, Jiang H, Li X, et al. (2008) Tract probability maps in stereotaxic spaces: analyses of white matter anatomy and tract-specific quantification. *NeuroImage* 39: 336-347.
20. Keihaninejad S, Ryan NS, Malone IB, Modat M, Cash D, et al. (2012) The importance of group-wise registration in tract based spatial statistics study of neurodegeneration: a simulation study in Alzheimer's disease. *PLoS One* 7: e45996.
21. Makris N, Papadimitriou GM, Sorg S, Kennedy DN, Caviness VS, et al. (2007) The occipitofrontal fascicle in humans: a quantitative, in vivo, DT-MRI study. *Neuroimage* 37: 1100-1111.
22. Shinoura N, Suzuki Y, Tsukada M, Katsuki S, Yamada R, et al. (2007) Impairment of inferior longitudinal fasciculus plays a role in visual memory disturbance. *Neurocase* 13: 127-130.
23. Papagno C, Miracapillo C, Casarotti A, Romero Lauro LJ, Castellano A, et al. (2011) What is the role of the uncinate fasciculus? Surgical removal and proper name retrieval. *Brain* 134: 405-414.
24. Chen WW, Wang N, Cai S, Fang Z, Yu M, et al. (2013) Structural brain abnormalities in patients with primary open-angle glaucoma: a study with 3T MR imaging. *Invest Ophthalmol Vis Sci* 54: 545-554.
25. Beaulieu C (2002) The basis of anisotropic water diffusion in the nervous system - a technical review. *NMR Biomed* 15: 435-455.
26. Gold BT, Johnson NF, Powell DK, Smith CD (2012) White matter integrity and vulnerability to Alzheimer's disease: preliminary findings and future directions. *Biochim Biophys Acta* 1822: 416-422.
27. Alves GS, O'Dwyer L, Jurcoane A, Oertel-Knochel V, Knochel C, et al. (2012) Different patterns of white matter degeneration using multiple diffusion indices and volumetric data in mild cognitive impairment and Alzheimer patients. *PloS one* 7: e52859.
28. Michelson G, Engelhorn T, Warntges S, El Rafei A, Hornegger J, et al. (2013) DTI parameters of axonal integrity and demyelination of the optic radiation correlate with glaucoma indices. *Graefes Arch Clin Exp Ophthalmol* 251: 243-253.
29. Fox RJ, Cronin T, Lin J, Wang X, Sakaie K, et al. (2011) Measuring myelin repair and axonal loss with diffusion tensor imaging. *AJNR Am J Neuroradiol* 32: 85-91.
30. Engelhorn T, Michelson G, Waerntges S, Otto M, El-Rafei A, et al. (2012) Changes of radial diffusivity and fractional anisotropy in the optic nerve and optic radiation of glaucoma patients. *ScientificWorldJournal* 2012: 849632.
31. Schoemann J, Engelhorn T, Waerntges S, Doerfler A, El-Rafei A, et al. (2014) Cerebral microinfarcts in primary open-angle glaucoma correlated with DTI-derived integrity of optic radiation. *Invest Ophthalmol Vis Sci* 55: 7241-7247.